

# Imaging Intraplaque Inflammation in Carotid Atherosclerosis With F-18-Fluorocholine Positron Emission Tomography-Computed Tomography Prospective Study on Vulnerable Atheroma With Immunohistochemical Validation

Citation for published version (APA):

Vöö, S., Kwee, R. M., Sluimer, J. C., Schreuder, F. H. B. M., Wierdsma, R., Bauwens, M., Heeneman, S., Cleutjens, J. P. M., van Oostenbrugge, R. J., Daemen, J-W. H., Daemen, M. J. A. P., Mottaghy, F. M., & Kooi, E. (2016). Imaging Intraplaque Inflammation in Carotid Atherosclerosis With F-18-Fluorocholine Positron Emission Tomography-Computed Tomography Prospective Study on Vulnerable Atheroma With Immunohistochemical Validation. *Circulation-Cardiovascular Imaging*, 9(5), Article e004467. <https://doi.org/10.1161/CIRCIMAGING.115.004467>

**Document status and date:**

Published: 01/05/2016

**DOI:**

[10.1161/CIRCIMAGING.115.004467](https://doi.org/10.1161/CIRCIMAGING.115.004467)

**Document Version:**

Publisher's PDF, also known as Version of record

**Document license:**

Taverne

**Please check the document version of this publication:**

- A submitted manuscript is the version of the article upon submission and before peer-review. There can be important differences between the submitted version and the official published version of record. People interested in the research are advised to contact the author for the final version of the publication, or visit the DOI to the publisher's website.
- The final author version and the galley proof are versions of the publication after peer review.
- The final published version features the final layout of the paper including the volume, issue and page numbers.

[Link to publication](#)

**General rights**

Copyright and moral rights for the publications made accessible in the public portal are retained by the authors and/or other copyright owners and it is a condition of accessing publications that users recognise and abide by the legal requirements associated with these rights.

- Users may download and print one copy of any publication from the public portal for the purpose of private study or research.
- You may not further distribute the material or use it for any profit-making activity or commercial gain
- You may freely distribute the URL identifying the publication in the public portal.

If the publication is distributed under the terms of Article 25fa of the Dutch Copyright Act, indicated by the "Taverne" license above, please follow below link for the End User Agreement:

[www.umlib.nl/taverne-license](http://www.umlib.nl/taverne-license)

**Take down policy**

If you believe that this document breaches copyright please contact us at:

[repository@maastrichtuniversity.nl](mailto:repository@maastrichtuniversity.nl)

providing details and we will investigate your claim.

Download date: 04 Oct. 2023

## Imaging Intraplaque Inflammation in Carotid Atherosclerosis With $^{18}\text{F}$ -Fluorocholine Positron Emission Tomography–Computed Tomography Prospective Study on Vulnerable Atheroma With Immunohistochemical Validation

Stefan Vöö, MD, PhD; Robert M. Kwee, MD, PhD; Judith C. Sluimer, PhD; Floris H. B. M. Schreuder, MD; Roel Wiers, MSc; Matthias Bauwens, PhD; Sylvia Heeneman, PhD; Jack P. M. Cleutjens, PhD; Robert J. van Oostenbrugge, MD, PhD; Jan-Willem H. Daemen, MD, PhD; Mat J. A. P. Daemen, MD, PhD; Felix M. Mottaghy, MD, PhD; M. Eline Kooi, PhD

**Background**— $^{18}\text{F}$ -fluorocholine ( $^{18}\text{F}$ -FCH) uptake is associated with cell proliferation and activity in tumor patients. We hypothesized that  $^{18}\text{F}$ -FCH could similarly be a valuable imaging tool to identify vulnerable plaques and associated intraplaque inflammation and atheroma cell proliferation.

**Methods and Results**—Ten consecutive stroke patients (90% men, median age 66.5 years, range, 59.4–69.7) with ipsilateral >70% carotid artery stenosis and who underwent carotid endarterectomy were included in the study. Before carotid endarterectomy, all patients underwent positron emission tomography to assess maximum  $^{18}\text{F}$ -FCH uptake in ipsilateral symptomatic carotid plaques and contralateral asymptomatic carotid arteries, which was corrected for background activity, resulting in a maximum target-to-background ratio (TBRmax). Macrophage content was assessed in all carotid endarterectomy specimens as a percentage of CD68<sup>+</sup>-staining per whole plaque area (plaqueCD68<sup>+</sup>) and as a maximum CD68<sup>+</sup> percentage (maxCD68<sup>+</sup>) in the most inflamed section/plaque. Dynamic positron emission tomography imaging demonstrated that an interval of 10 minutes between  $^{18}\text{F}$ -FCH injection and positron emission tomography acquisition is appropriate for carotid plaque imaging. TBRmax in ipsilateral symptomatic carotid plaques correlated significantly with plaqueCD68<sup>+</sup> (Spearman's  $\rho=0.648$ ,  $P=0.043$ ) and maxCD68<sup>+</sup> ( $\rho=0.721$ ,  $P=0.019$ ) in the 10 corresponding carotid endarterectomy specimens. TBRmax was significantly higher ( $P=0.047$ ) in ipsilateral symptomatic carotid plaques (median: 2.0; interquartile range [Q1–Q3], 1.5–2.5) compared with the contralateral asymptomatic carotid arteries (median: 1.4; Q1–Q3, 1.3–1.6). TBRmax was not significantly correlated to carotid artery stenosis ( $\rho=0.506$ ,  $P=0.135$ ).

**Conclusions**—In vivo uptake of  $^{18}\text{F}$ -FCH in human carotid atherosclerotic plaques correlated strongly with degree of macrophage infiltration and recent symptoms, thus  $^{18}\text{F}$ -FCH positron emission tomography is a promising tool for the evaluation of vulnerable plaques.

**Clinical Trial Registration**—URL: <http://www.clinicaltrials.gov>. Unique identifier: NCT01899014. (*Circ Cardiovasc Imaging*. 2016;9:e004467. DOI: 10.1161/CIRCIMAGING.115.004467.)

**Key Words:** atherosclerosis ■ carotid artery diseases ■ endarterectomy ■ fluorocholine  
■ inflammation ■ macrophages ■ positron-emission tomography

Carotid endarterectomy (CEA) has been shown to prevent stroke in patients with high-grade carotid artery stenosis.<sup>1</sup> It has, however, become increasingly clear that the degree of luminal stenosis alone is not the most optimal clinical decision parameter. Patients with almost occluded carotid arteries may remain completely asymptomatic throughout their lifetime,

See Editorial by Toczek and Sadeghi  
See Clinical Perspective

whereas strokes may occur in the absence of severe carotid stenosis because of outward arterial remodeling of a vulnerable plaque.<sup>2</sup> Hence, novel targets for noninvasive imaging of

Received August 18, 2015; accepted March 17, 2016.

From the CARIM School for Cardiovascular Diseases, Maastricht, The Netherlands (S.V., J.C.S., F.H.B.M.S., S.H., R.J.v.O., M.E.K.); Departments of Radiology and Nuclear Medicine (S.V., R.M.K., F.H.B.M.S., R.W., M.B., F.M.M., M.E.K.), Pathology (J.C.S., S.H., J.P.M.C.), Neurology (F.H.B.M.S., R.J.v.O.), and Surgery (J.-W.H.D.), Maastricht University Medical Center (MUMC), Maastricht, The Netherlands; Department of Pathology, Academic Medical Center, Amsterdam, The Netherlands (M.J.A.P.D.); and Department of Nuclear Medicine, University Hospital, RWTH Aachen University, Aachen, Germany (F.M.M.).

The Data Supplement is available at <http://circimaging.ahajournals.org/lookup/suppl/doi:10.1161/CIRCIMAGING.115.004467/-/DC1>.

Correspondence to M. Eline Kooi, PhD, Department of Radiology and Nuclear Medicine, Maastricht University Medical Center, P. Debyealaan 25, PO Box 5800, 6202AZ Maastricht, The Netherlands. E-mail [eline.kooi@mumc.nl](mailto:eline.kooi@mumc.nl) or Felix M. Mottaghy, MD, PhD, Department of Nuclear Medicine, University Hospital, RWTH Aachen, Pauwelsstr. 30, D-52072 Aachen, Germany. E-mail [fmottaghy@ukaachen.de](mailto:fmottaghy@ukaachen.de)

© 2016 American Heart Association, Inc.

*Circ Cardiovasc Imaging* is available at <http://circimaging.ahajournals.org>

DOI: 10.1161/CIRCIMAGING.115.004467

vulnerable plaques are absolutely required for reliable patient risk stratification.

The composition and biological activity of plaques have emerged as important determinants of cerebrovascular events alongside the degree of luminal narrowing.<sup>3</sup> Intraplaque inflammation plays a key role in the progression and destabilization of atherosclerotic lesions<sup>4,5</sup> and has been proposed as a major criterion for defining a high-risk vulnerable plaque.<sup>3-5</sup>

Positron emission tomography (PET) with the tracer <sup>18</sup>F-fluoro-2-deoxy-D-glucose (<sup>18</sup>F-FDG) allows measurement of metabolic activity and tends to correlate with plaque macrophage infiltration,<sup>6-8</sup> cardiovascular risk factors,<sup>9</sup> Framingham Risk Score,<sup>10</sup> and recent symptoms.<sup>11,12</sup> However, <sup>18</sup>F-FDG PET of atherosclerotic plaques remains challenging because of intense background FDG uptake that can potentially swamp any plaque signal<sup>13-15</sup> and of some technical disadvantages, which include reduced cellular <sup>18</sup>F-FDG uptake in hyperglycemia,<sup>14,15</sup> the need to fast for ≥6 hours before <sup>18</sup>F-FDG injection,<sup>13</sup> and a lengthy waiting time of 2.5 to 3 hours between <sup>18</sup>F-FDG injection and image acquisition to achieve an optimal vessel wall to background ratio.<sup>15</sup>

The newer <sup>18</sup>F-fluorocholine (<sup>18</sup>F-FCH) tracer may be an attractive alternative to <sup>18</sup>F-FDG. Choline is a key precursor of phosphatidylcholine (lecithin), a major phospholipid component of all cellular membranes, and thus it is closely associated with cellular proliferation and activity.<sup>16</sup> Radiolabeled-choline PET tracers (including <sup>18</sup>F-FCH) are highly taken up by tumor cells<sup>17</sup> and also by active and proliferating macrophages involved in inflammatory processes.<sup>18-21</sup> A retrospective trial of tumor patients also assessing carotid atherosclerosis has shown a significantly increased choline uptake in noncalcified regions, assumed to be inflamed plaques, in comparison to the healthy vessel wall.<sup>22</sup> Interestingly, in a side-by-side comparison between <sup>18</sup>F-FCH and <sup>18</sup>F-FDG in murine atherosclerotic lesions, choline uptake correlated with macrophage staining even better than FDG uptake.<sup>20</sup> However, it is yet unknown whether <sup>18</sup>F-FCH uptake in plaques is associated with symptoms in cardiovascular patients and histological markers of plaque vulnerability.

Therefore, in this proof-of-principle study, we prospectively investigated whether <sup>18</sup>F-FCH PET can be used to assess vulnerable plaque macrophage infiltration and whether the degree of <sup>18</sup>F-FCH uptake can be used to discriminate between recently symptomatic and asymptomatic lesions.

## Methods

### Ethical Considerations

The present article is a prospective, cross-sectional diagnostic study with patient inclusion conforming to the principles outlined in the Helsinki Declaration II. All patients gave written informed consent before inclusion in the study. The study protocol was approved by the ethical committee of the Maastricht University Medical Center (METC13-2-015), registered at the European and Dutch referral committees on research involving human subjects (EUDRACT2013-000456-17/NL43466.068.13) and in the clinical trials registry ClinicalTrials.gov (NCT01899014). Radiation exposure was licensed by the local radiation safety committee and study monitoring was performed by the Clinical Trial Center Maastricht.

### Patients

The study included 10 consecutive patients after onset of acute cerebrovascular event (stroke, transient ischemic event, or amaurosis

fugax) who were scheduled for CEA because of severe ipsilateral carotid artery stenosis. All patients were clinically assessed by an experienced vascular neurologist or vascular surgeon at the stroke unit or the Cardiovascular Outpatient Clinic (Maastricht University Medical Center). All patients were symptomatic at the ipsilateral side of carotid artery stenosis, defined as cerebrovascular symptoms in the ipsilateral anterior cerebral circulation or the retinal circulation, in combination with a 70% to 99% stenosis of the carotid artery, according to the North American Symptomatic Carotid Endarterectomy Trial criteria.<sup>1</sup> Before enrollment, the degree of carotid stenosis on the ipsilateral and contralateral side was assessed by experienced ultrasonographers using Doppler-ultrasonography.<sup>23</sup> Carotid stenosis was categorized as follows: normal, <50%, 50% to 69%, 70% to 99% stenosis, and total occlusion. Exclusion criteria included pregnancy, breastfeeding mothers, contraindications to iodinated contrast agents including known intolerance to contrast agents or impaired renal function (renal clearance <45 mL/min/1.73 m<sup>2</sup> or <60 mL/min/1.73 m<sup>2</sup> in patients with diabetes mellitus), serious clinical conditions (dementia, severe heart failure New York Heart Association class III-IV, and severe pulmonary dysfunction dependent of oxygen supply), or major neurological deficits (hemiparesis, complete aphasia). Clinical history and medication use were ascertained at the time of subject enrollment. Study participants underwent carotid <sup>18</sup>F-FCH PET-computed tomography (CT) within 14 days before CEA.

### <sup>18</sup>F-FCH Positron Emission Tomography–Computed Tomography Protocol

The synthesis of <sup>18</sup>F-FCH was based on a previously described protocol<sup>24</sup> and performed according to the European directive on radiopharmaceuticals.

PET-CT (positron emission tomography–computed tomography) imaging of both carotid arteries was performed on a Gemini TF-64 PET-CT scanner (Philips Healthcare, Best, The Netherlands). Starting simultaneously with the intravenous injection of <sup>18</sup>F-FCH (4 MBq/kg body weight), 30-minute dynamic PET imaging was performed (3-dimensional mode, 1-bed position), with field-of-view centered at the carotid artery bifurcation. Additional static PET images were taken 60 minutes post <sup>18</sup>F-FCH injection. Then, contrast-enhanced CT images were obtained by using 90 mL of iobitridol (Supplemental Methods in the Data Supplement).

### CEA and Histology Preparation

Surgeons were instructed to remove the carotid plaques in one piece. After CEA, the carotid plaques were immediately fixed in 10% buffered formalin. Carotid plaques were transversely cut in 4-mm slices, decalcified, embedded in paraffin, and transversely cut in 4- $\mu$ m sections, as previously described.<sup>25</sup> Adjacent 4- $\mu$ m sections were subjected to immunohistological staining with monoclonal antibodies against: CD68, for identification of macrophages; human alveolar macrophage marker-56 (HAM56), for confirmatory macrophage content analysis; major histopathology complex class-II (MHC-II), for activated inflammatory cells; or IgG control (Supplemental Methods in the Data Supplement).

### Coregistration of the Ipsilateral Symptomatic Carotid Plaque at PET-CT With Histology

Anatomic colocalization between corresponding PET-CT slices on the ipsilateral symptomatic side and histopathologic sections was performed by locating plaques relative to the carotid bifurcation and the narrowest carotid artery lumen as landmarks, as previously described (Supplemental Methods in the Data Supplement).<sup>25</sup>

### <sup>18</sup>F-FCH PET-CT Evaluation

Carotid <sup>18</sup>F-FCH uptake, expressed as standardized uptake value (SUV), was measured at 4-mm intervals along the length of the carotid artery on a dedicated workstation with dedicated fusion software (Syntegra, Philips Healthcare). Carotid plaque was identified on contrast-enhanced CT images, defined as thickening of the vessel



wall and calcification, and carotid stenosis grade was assessed using the North American Symptomatic Carotid Endarterectomy Trial method.<sup>11</sup>

On the ipsilateral symptomatic side, circular regions of interests (ROIs) were placed on consecutive axial CT images encompassing the outer carotid vessel wall at the level of the plaque (Figure 1).

On the contralateral asymptomatic side, ROIs were placed similarly along the carotid plaque when this was identified on contrast-enhanced CT. When no plaque was identified on asymptomatic sides, circular ROIs were placed on consecutive axial CT images encompassing the outer vessel wall from the internal carotid artery (8 mm cranial of the carotid bifurcation) to the level of the common carotid artery (12 mm caudal of the carotid bifurcation).

For each slice, the maximum SUV was measured as the maximum pixel activity within ROI. The maximum value of all SUVs (SUVmax) was recorded for both the symptomatic carotid plaque and the asymptomatic carotid artery. Finally, the carotid SUVmax values were corrected for blood activity by dividing by the average blood activity obtained from five circular 6-mm diameter ROIs placed in the center of the subclavian or internal jugular vein on consecutive axial CT images (SUVmean venous blood). The resulting blood-corrected values were expressed as maximum target-to-background ratio (TBRmax). PET images were reported in consensus by a nuclear medicine physician–nuclear cardiologist (>4 years of experience, with >2 years of experience at quantifying carotid plaque on PET) and a nuclear medicine physician with extensive PET experience (>10 years experience) and cardiovascular interest.

### Histological Analysis

Using high-resolution digital microscopy, total plaque area and CD68<sup>+</sup> macrophage content were quantified at each 4- $\mu$ m section using a computer-assisted color image analysis (QWin V3; Leica, Cambridge, England).<sup>26</sup> Macrophage content was expressed as percentage of CD68<sup>+</sup> area to total plaque area (plaqueCD68<sup>+</sup>). The

maximum macrophage content was determined at the plaque section with the highest CD68<sup>+</sup> percentage (maxCD68<sup>+</sup>).

Histological analysis was performed by a trained reader (>1 year experience in histological plaque assessment), blinded to clinical and PET data. To determine the variability of the CD68<sup>+</sup> content measurement, the images were reanalyzed by the same observer 3 months apart in a masked manner. The intraclass correlation coefficient was 0.92 (95% confidence interval, 0.81–0.98).

### Tritiated Choline Uptake Assay

Choline uptake by activated macrophages was assessed using a protocol adapted from Folco et al.<sup>27</sup> Human monocytic cells (human acute monocytic leukemia cell line) were differentiated to macrophages. To induce cell activation, macrophages were incubated in RPMI1640 medium, followed by the addition of lipopolysaccharide, tumor necrosis factor- $\alpha$ , and interferon- $\gamma$ . Nonactivated macrophages served as controls.

Cells were first washed with phosphate-buffered saline. <sup>3</sup>H-choline was added to the cells and incubated for 30 minutes at 37°C. Cells were washed twice and detached, counted, and further assayed by liquid scintillation counting (Beckman LS 6000IC counter). The net uptake of <sup>3</sup>H-choline is expressed as counts of choline/cell/min (Supplemental Methods in the Data Supplement).

### Statistical Analysis

Statistical analyses were performed using IBM SPSS Statistics for Windows, Version 22.0 (IBM Corporation, Armonk, NY). Differences in <sup>18</sup>F-FCH activity at various time points and differences between symptomatic and asymptomatic carotid arteries were assessed by Wilcoxon signed-rank tests. The study is underpowered to assess the effect of cardiovascular risk factors and medication on choline uptake. However, in light of statin's known anti-inflammatory effect, the available data provided an opportunity to screen for a potential

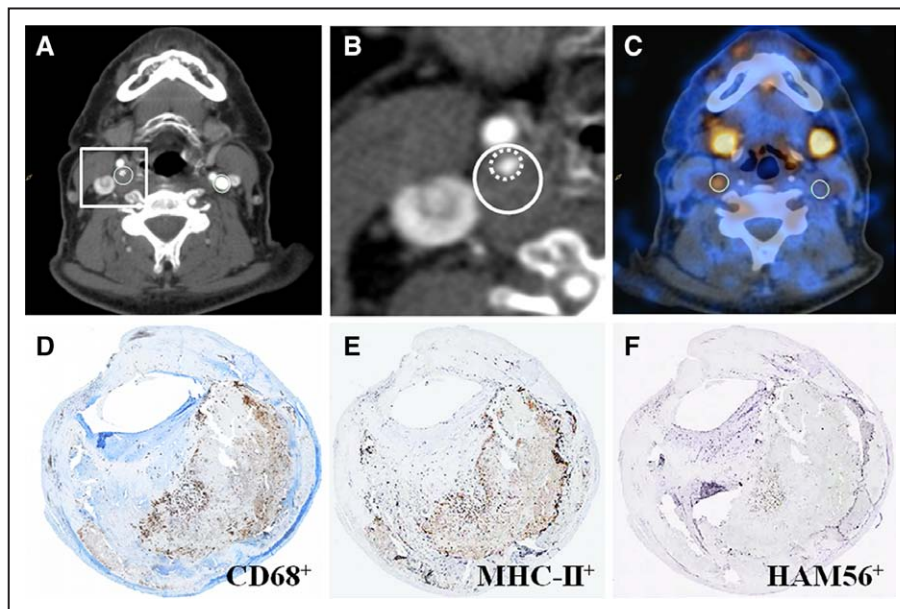


**Figure 1.** Representative <sup>18</sup>F-fluorocholine positron emission tomography-computed tomography (<sup>18</sup>F-FCH PET-CT) images and corresponding histology of a symptomatic and contralateral asymptomatic carotid plaque of a 67-year-old patient who experienced right-sided stroke 12 days before PET-CT imaging. **A**, Diagnostic contrast-enhanced CT shows a significant stenosis in the right internal carotid artery because of a soft plaque, whereas no atherosclerotic plaque can be seen on the contralateral internal carotid artery. Regions of interest (ROI, white outlining) drawn around the outer border of the vessel walls were placed along the right carotid stenosis and along the contralateral carotid artery, respectively. **B**, CT, inset on the symptomatic plaque. **C**, The fused PET-CT image denotes a focal area of high <sup>18</sup>F-FCH uptake in the ROI drawn onto the right symptomatic carotid plaque, whereas there is no visible <sup>18</sup>F-FCH uptake in the left asymptomatic carotid plaque. The activity recorded for both symptomatic and contralateral asymptomatic carotid arteries were corrected for venous blood background activity in the jugular veins, resulting in a maximum target-to-background ratio of 2.46 and 1.18, respectively. Corresponding immunohistochemistry sections indicating CD68<sup>+</sup> (**D**), MHC-II<sup>+</sup> (**E**), and HAM56<sup>+</sup> (**F**) cells (all in brown). MHC-II indicates major histopathology complex class-II; HAM56, human alveolar macrophage marker-56.

influence of statins on choline uptake. Thus, a subgroup analysis was performed, whereby  $^{18}\text{F}$ -FCH activity was assessed according to long-term statin use. Differences between different subgroups were assessed by using a Mann–Whitney  $U$  test. Correlations between  $^{18}\text{F}$ -FCH uptake and histological degree of macrophage infiltration or degree of arterial stenosis (on contrast-enhanced CT) were assessed by the Spearman rank correlation test. A two-sided  $P < 0.05$  was considered statistically significant.

## Results

### Baseline Characteristics

Patient characteristics are displayed in Table 1. Median interval between last symptoms (amaurosis fugax,  $n=5$ ; transient ischemic attack,  $n=2$ ; and minor nondisabling stroke,  $n=3$ ) and  $^{18}\text{F}$ -FCH PET was 11 (Q1–Q3, 9–12) days. Median interval between  $^{18}\text{F}$ -FCH PET and CEA was 2 (Q1–Q3, 1–3) days.

### Carotid Artery Stenosis Grade

Symptomatic carotid arteries had significantly higher stenosis grade than contralateral asymptomatic carotid arteries (median: 97.5%, Q1–Q3: 94.0–99.0% versus 70%, Q1–Q3: 20.0–95.0%, respectively;  $P=0.019$ ; Table 2).

### Uptake and Dynamics of $^{18}\text{F}$ -FCH

Representative PET and histological images are shown in Figure 1 and Figure I in the Data Supplement.

**Table 1. Baseline Characteristics of the Included Subjects (n=10)**

Characteristic	Value
Age, y (median, Q1–Q3)	66.5 (59.4–69.7)
Male sex	9 (90.0%)
Caucasian race	10 (100.0%)
Prior medical history	
Ischemic cerebrovascular and/or cardiovascular disease	3 (30.0%)
Current or previous smoking	8 (80.0%)
Arterial hypertension	9 (90.0%)
Hyperlipidemia	9 (90.0%)
Diabetes mellitus	3 (30.0%)
Number of cardiovascular risk factors	
≥4	8 (80.0%)
2–3	2 (20.0%)
Concurrent neurological symptoms	
Minor stroke, transient ischemic attack, or amaurosis fugax	10 (100%)
Medication	
Antiplatelet agent	10 (100.0%)
Antihypertensive agent	7 (70.0%)
Statin*	10 (100.0%)

Data are presented as numbers and percentages between brackets, unless otherwise indicated. Q1–Q3 indicates interquartile range.

\* $n=4$ , duration >6 months.

Expression of CD68, a pan-macrophage marker, and the macrophage activation marker MHC-II largely colocalized with  $^{18}\text{F}$ -FCH uptake in the symptomatic plaques, while expression of the human alveolar macrophage marker-56, as a second confirmatory macrophage marker, was more restricted (Figure 1).

Dynamic PET imaging demonstrated that background blood pool activity peaked immediately post  $^{18}\text{F}$ -FCH injection (median SUVmean: 9.7, Q1–Q3: 7.8–16.7). It dropped rapidly within 3 minutes ( $T_{1/2}=3$  minutes, median SUVmean: 1.3, Q1–Q3: 1.1–1.4) reaching a steady-state already at 10 minutes (median SUVmean: 1.03, Q1–Q3: 0.9–1.1) postinjection (Figure 2).

In both the symptomatic as well as contralateral asymptomatic plaques, dynamic PET imaging showed an initial peak activity (median SUVmax: 12.8, Q1–Q3: 12.0–16.4 and 13.1, Q1–Q3: 10.4–16.1, respectively), which was mostly attributed to the  $^{18}\text{F}$ -FCH bolus and which, similar to blood pool activity, rapidly dropped within 3 minutes. Activity in the symptomatic and asymptomatic carotid plaques reached a steady-state level 10 minutes post  $^{18}\text{F}$ -FCH injection (median SUVmax: 2.0, Q1–Q3: 1.6–2.3 and 1.5, Q1–Q3: 1.1–1.6, respectively; Figure 2).

**Table 2. Carotid Artery Stenosis Grade of Ipsilateral Symptomatic and Contralateral Asymptomatic Carotid Arteries in All Subjects (n=10)**

Characteristic	Ipsilateral Symptomatic Carotid Artery	Contralateral Asymptomatic Carotid Artery
Plaque stenosis on contrast-enhanced CT (median, Q1–Q3)	97.5% (94.0–99.0%)	70.0% (20.0–95.0%)
Carotid plaque on Doppler ultrasonography		
Absence of plaque	0 (0%)	2 (20.0%)
<50% stenosis	0 (0%)	2 (20.0%)
50% to 69% stenosis	0 (0%)	2 (20.0%)
70% to 99% stenosis	10 (100.0%)	3 (30.0%)
Occlusion	0 (0%)	1 (10.0%)
$^{18}\text{F}$ -FCH PET		
TBRmax (median, Q1–Q3)	2.00 (1.46–2.49)	1.39 (1.27–1.61)
SUVmean venous blood (median, Q1–Q3)	1.03 (0.98–1.14)	0.98 (0.90–1.09)
CD68 <sup>+</sup> immunohistochemistry		
PlaqueCD68 <sup>+</sup> , % (median, Q1–Q3)	5.6% (2.3–8.7%)	NA
MaxCD68 <sup>+</sup> , % (median, Q1–Q3)	10.5% (4.9–15.4%)	NA
Total plaque area, mm <sup>2</sup> (median, Q1–Q3)	129.5 (85.7–171.3)	NA

Data are presented as numbers and percentages between brackets, unless otherwise indicated. CT indicates computed tomography;  $^{18}\text{F}$ -FCH PET,  $^{18}\text{F}$ -fluorocholine positron emission tomography; NA, not assessed; Q1–Q3, interquartile range; SUV, standard uptake value; and TBRmax, maximum target-to-background ratio.

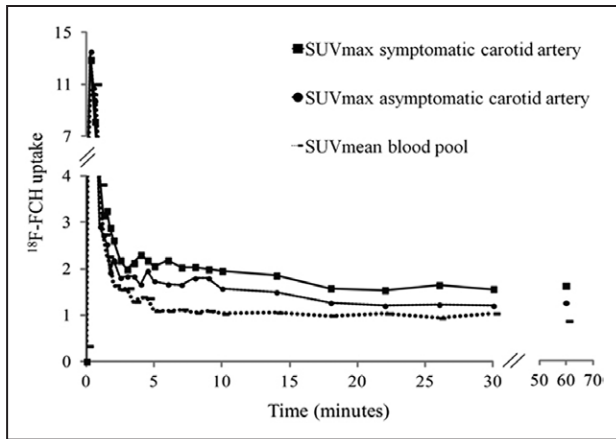


**Figure 2.** Dynamic tracer uptake. Graph showing  $^{18}\text{F}$ -FCH uptake in the blood pool and in the ipsilateral symptomatic carotid plaques during the first 60 minutes after tracer injection ( $n=10$ ). After  $^{18}\text{F}$ -FCH injection,  $^{18}\text{F}$ -FCH blood pool activity dropped rapidly ( $T_{1/2}=3$  minutes), whereas the activity in the symptomatic and asymptomatic carotid plaques stabilized rapidly already at 10 minutes postinjection.  $^{18}\text{F}$ -FCH indicates  $^{18}\text{F}$ -fluorocholine; and SUV, standardized uptake value.

### Correlation Between $^{18}\text{F}$ -FCH Uptake in Symptomatic Carotid Plaques and Histology

$\text{CD68}^+$  macrophage content varied markedly between patients (Table 2). TBRmax in symptomatic carotid plaques 10 minutes post  $^{18}\text{F}$ -FCH injection correlated strongly with the plaque  $\text{CD68}^+$  macrophage content ( $\rho=0.648$ ,  $P=0.043$ ) and max  $\text{CD68}^+$  ( $\rho=0.721$ ,  $P=0.019$ ; Figure 3).

In vitro tritiated-choline experiments showed that the choline uptake rate increases  $>5$ -folds in human monocyte-derived macrophages under proinflammatory stimulation compared with the unstimulated cells (median: 1.1, Q1–Q3: 0.8–1.2 versus 0.2, Q1–Q3: 0.1–0.3 nmol/cell/h, respectively;  $P=0.009$ ).

### Comparison of Symptomatic Carotid Plaques With Contralateral Asymptomatic Arteries

TBRmax 10 minutes post  $^{18}\text{F}$ -FCH injection was significantly higher ( $P=0.047$ ) in the symptomatic carotid plaques (median:

2.0, Q1–Q3: 1.5–2.5) compared with the contralateral arteries (median: 1.4, Q1–Q3: 1.3–1.6; Figure 4).  $^{18}\text{F}$ -FCH uptake was not significantly related to carotid artery stenosis grade, for both the symptomatic ( $\rho=0.506$ ,  $P=0.135$ ) and asymptomatic side ( $\rho=0.413$ ,  $P=0.207$ ).

As statin therapy was initiated after the index event, 6 patients were on statins  $<15$  days, whereas 4 patients with a history of cardiovascular disease were on statins  $>6$  months. Our results showed a tendency toward a lower choline uptake in patients  $>6$  month under statin-treatment compared with those  $<15$  days under therapy (TBRmax median: 1.6, Q1–Q3: 1.2–1.9 versus 2.3, Q1–Q3: 1.3–2.6, respectively;  $P=0.055$ ). No such difference was observed at the asymptomatic side.

## Discussion

Here we have demonstrated that  $^{18}\text{F}$ -FCH PET is a valuable tool for imaging of vulnerable atherosclerotic plaques. Irrespective of the degree of carotid artery stenosis,  $^{18}\text{F}$ -FCH uptake significantly correlated with plaque macrophage content, a measure of plaque inflammation and vulnerability, and could distinguish between recently symptomatic vulnerable plaques and asymptomatic plaques.

Choline is an essential precursor of phospholipids, a key substrate of cell membranes.<sup>16</sup> Hence, high membrane turnover in proliferating and in active cells is closely associated with an increased choline metabolism.<sup>17–19</sup> Radiolabeled-choline tracers are already used in clinical PET imaging of different cancers<sup>17</sup> and are under evaluation for imaging of different inflammatory conditions.<sup>18,19</sup> We showed enhanced  $^{18}\text{F}$ -FCH uptake in human carotid plaques early after onset of a cerebrovascular event compared with a low uptake in asymptomatic plaques. Previous reports, limited to a retrospective analysis of patients who underwent PET imaging for prostate cancer, have described choline uptake in the aorta and carotid arteries.<sup>22,28,29</sup> As choline uptake was found mainly in noncalcified vessel wall areas,<sup>22</sup> these reports raised the possibility of choline uptake in vulnerable atherosclerotic plaques. However, no clear conclusion could

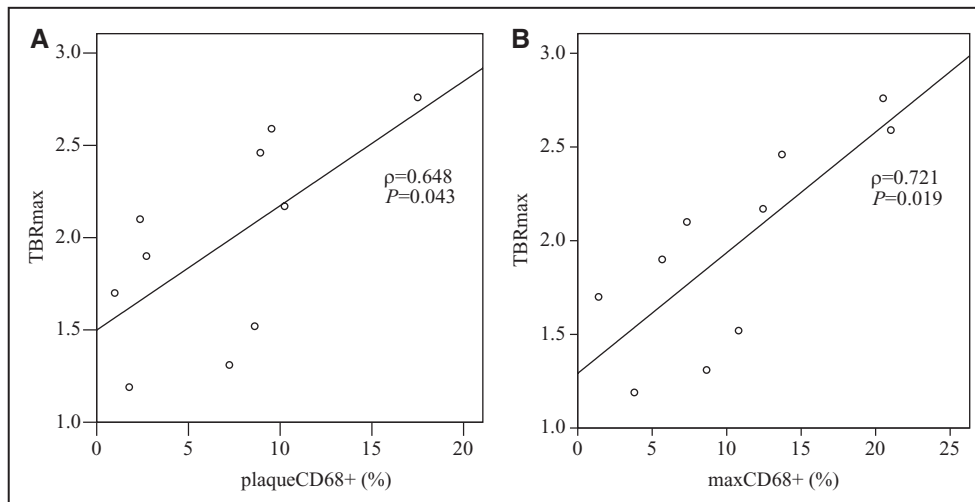


**Figure 3.** Correlation of tracer uptake and immunohistochemistry. Graphs showing the correlation between TBRmax in symptomatic carotid plaques 10 minutes after  $^{18}\text{F}$ -fluorocholine injection and plaque  $\text{CD68}^+$  (A) and max  $\text{CD68}^+$  (B) of the 10 corresponding carotid end-arterectomy specimens. TBRmax indicates maximum target-to-background ratio.

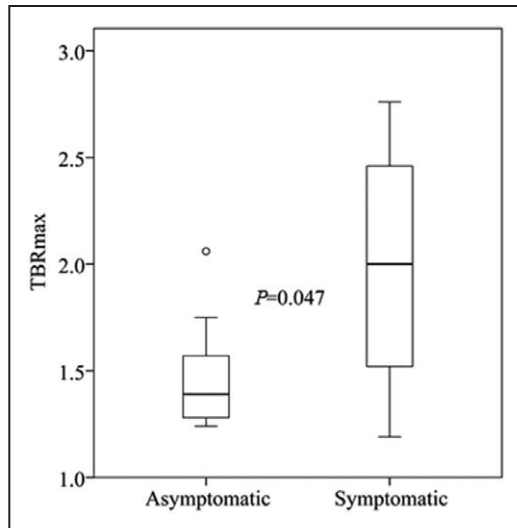


**Figure 4.** Correlation of tracer uptake and patient symptoms. Box-plots of TBRmax 10 minutes after  $^{18}\text{F}$ -fluorocholine injection in ipsilateral symptomatic carotid plaques vs contralateral asymptomatic carotid arteries. Line represents median, box 25th to 75th percentile, and the whiskers 5th to 95th percentile. TBRmax indicates maximum target-to-background ratio.

be drawn from these reports because of their retrospective nature and lack of histological validation.

Another novel aspect of the present study is the correlation between  $^{18}\text{F}$ -FCH uptake in symptomatic human plaques with immunohistological analysis of plaque vulnerability, as a gold standard. The level of  $^{18}\text{F}$ -FCH uptake in the symptomatic carotid plaques strongly correlated with the degree of intraplaque CD68<sup>+</sup> macrophage content, a surrogate marker of intraplaque inflammation and vulnerability. This finding is in agreement with previous experimental animal data showing a high choline uptake in inflamed plaques,<sup>20,21</sup> which strongly correlates with the amount of active intraplaque macrophages.<sup>20</sup> The enhanced choline uptake may be explained by high macrophage proliferation present in symptomatic CEA specimens,<sup>30</sup> or by enhanced choline transporter expression and choline kinase activity, as seen under inflammatory conditions.<sup>31</sup> Furthermore, choline kinase activity is significantly increased by hypoxia or under stimulation with tumor necrosis factor- $\alpha$ ,<sup>31</sup> which are both present in vulnerable plaques<sup>4</sup> and may hence explain high  $^{18}\text{F}$ -FCH uptake.

Interestingly, in a mouse model of atherosclerosis it has been demonstrated that vulnerable plaque detection is more sensitive with  $^{18}\text{F}$ -FCH than with FDG (84% versus 64%).<sup>20</sup> The PET tracer FDG, a biological glucose analogue, has been extensively evaluated for measuring intraplaque inflammation in atherosclerotic plaques.<sup>6–12</sup> However, because FDG is taken up by any metabolically active tissues, including those surrounding atherosclerotic plaques (such as fat, muscles, and lymph nodes), concerns have been raised about the specificity of this tracer for imaging inflammatory cells. Indeed, Davies et al<sup>32</sup> showed that in vivo FDG uptake in atherosclerotic lesions of rabbit aorta does not correlate with macrophage density. They reported no significant difference in FDG uptake between rabbits with highly inflamed aortic walls, those with low levels of inflammation, or controls.<sup>32</sup> Moreover, recent

clinical data on FDG PET showed an inconsistent correlation between FDG uptake and intraplaque inflammation, ranging from significantly high,<sup>7</sup> medium,<sup>33</sup> to very poor correlation coefficients.<sup>34</sup> Conversely, a high degree of choline uptake in macrophage-rich areas of murine atherosclerotic lesions has been observed with choline in autoradiographic studies,<sup>20</sup> suggesting that  $^{18}\text{F}$ -FCH may provide a more specific tracer to assess active macrophage infiltration. However, no definitive conclusion on the relative specificity of the aforementioned tracers can be drawn until a direct head-to-head comparison is performed.

In terms of technical advantages for imaging atherosclerotic plaques by PET,  $^{18}\text{F}$ -FCH may provide significant advantages over  $^{18}\text{F}$ -FDG. First, no period of fasting before injection is required. Second,  $^{18}\text{F}$ -FCH clears from the blood rapidly, with little change in biodistribution pattern >10 minutes post injection.<sup>24</sup> Accordingly, our dynamic PET imaging data showed that blood pool activity dropped rapidly within 3 minutes, and that carotid plaque activity reached a steady state already after 10 minutes post  $^{18}\text{F}$ -FCH injection. Thus,  $^{18}\text{F}$ -FCH has a much shorter circulation time compared with  $^{18}\text{F}$ -FDG (10 minutes versus 2.5 hours). These advantages of  $^{18}\text{F}$ -FCH PET would increase patient comfort and throughput. Third, for diabetic patients,  $^{18}\text{F}$ -FCH uptake is not affected by prescan blood glucose levels that could hamper  $^{18}\text{F}$ -FDG uptake in these patients.<sup>14,15</sup>

A potential drawback to the use of  $^{18}\text{F}$ -FCH is that it is not yet FDA registered or approved despite its use in clinical oncological imaging. Yet whereas  $^{18}\text{F}$ -FCH is not yet available in the US, it is increasingly used throughout Europe, although to a lesser clinical extent and at higher prices compared with FDG. A concern is that despite having a much lower background uptake than FDG, the intense normal choline uptake in the salivary glands and oral mucosa may interfere with choline uptake at carotid bifurcation or in the internal carotid artery. We observed no such interference in the present study.

Future prospective studies are needed to investigate whether  $^{18}\text{F}$ -FCH PET can predict future strokes and improve risk stratification in patients with carotid atherosclerosis. In addition, the value of  $^{18}\text{F}$ -FCH uptake compared with other imaging markers of vulnerable plaques should be determined. These techniques include  $^{18}\text{F}$ -NaF PET for active plaque microcalcifications,<sup>35,36</sup>  $^{18}\text{F}$ -labeled Arginine-Glycine-Aspartic acid (RGD) peptides PET for intraplaque microvascularization;<sup>37</sup> and magnetic resonance imaging to visualize intraplaque hemorrhage, fibrous cap status, lipid-rich necrotic core size, and microvessel density.<sup>38</sup> As it remains unclear whether inflammation, microcalcification, or other vulnerable plaque features are the best for predicting clinical events, a double  $^{18}\text{F}$ -NaF and  $^{18}\text{F}$ -FCH PET assessment or combined  $^{18}\text{F}$ -FCH PET-magnetic resonance imaging are interesting imaging approaches to be tested in future clinical studies.

The present article was conceived as a proof-of-principle study and, therefore, its results cannot be extrapolated to a general population with carotid artery disease. Moreover, we acknowledge our study involves a relatively small number of patients. Hence, the effects of other possible determinants on  $^{18}\text{F}$ -FCH uptake, including injected  $^{18}\text{F}$ -FCH dose, medication, and renal function, could not be investigated as



they warrant larger prospective trials. Moreover, we did not perform a direct comparison between <sup>18</sup>F-FCH and <sup>18</sup>F-FDG PET, which is the current imaging standard for noninvasive assessment of inflammation in atherosclerosis. The added radiation dose from PET and CT remains an important concern. However, the total effective radiation dose in our patients was well below 10 mSv and comparable to a standard cardiac FDG PET-CT scan.

In conclusion, the present study provides proof of concept that <sup>18</sup>F-FCH PET of human carotid atherosclerotic plaques can distinguish between recently symptomatic and asymptomatic plaques and that <sup>18</sup>F-FCH uptake strongly correlates with degree of macrophage infiltration, a marker of plaque vulnerability. Our proof-of-principle study shows that <sup>18</sup>F-FCH PET can be a valuable tool to identify vulnerable carotid plaques and needs to be investigated in larger prospective studies.

### Acknowledgments

The authors thank Marielle Visser, BSc (Departments of Radiology and Nuclear Medicine, Maastricht University Medical Center), for her help with image acquisition and processing; Anique Janssen-Vrehen, BSc, Clairly Dinjens, BSc, Carla Langejan, BSc, Cécile Coumas-Stallinga, BSc (Department of Pathology, Maastricht University Medical Center, Maastricht), and Claire Mackaaij, BSc (Department of Pathology, Academic Medical Center, Amsterdam), for help with histological processing.

### Sources of Funding

This research was performed within the framework of the Center of Translational Molecular Medicine, Assessment of Plaque at Risk by Non-invasive (Molecular) Imaging and Modeling (ParisK) project (Grant OIC-202) ([www.ctmm.nl](http://www.ctmm.nl)), and was supported by a grant from the Dutch Heart Foundation. Dr Kooi is supported by Stichting De Weijerhorst.

### Disclosures

None.

### References

- Barnett HJ, Taylor DW, Eliasziw M, Fox AJ, Ferguson GG, Haynes RB, Rankin RN, Clagett GP, Hachinski VC, Sackett DL, Thorpe KE, Meldrum HE, Spence JD. Benefit of carotid endarterectomy in patients with symptomatic moderate or severe stenosis. North American Symptomatic Carotid Endarterectomy Trial Collaborators. *N Engl J Med*. 1998;339:1415–1425. doi: 10.1056/NEJM199811123392002.
- Halliday A, Mansfield A, Marro J, Peto C, Peto R, Potter J, Thomas D; MRC Asymptomatic Carotid Surgery Trial (ACST) Collaborative Group. Prevention of disabling and fatal strokes by successful carotid endarterectomy in patients without recent neurological symptoms: randomised controlled trial. *Lancet*. 2004;363:1491–1502. doi: 10.1016/S0140-6736(04)16146-1.
- Naghavi M, Libby P, Falk E, Casscells SW, Litovsky S, Rumberger J, Badimon JJ, Stefanadis C, Moreno P, Pasterkamp G, Fayad Z, Stone PH, Waxman S, Raggi P, Madjid M, Zarrabi A, Burke A, Yuan C, Fitzgerald PJ, Siscovick DS, de Korte CL, Aikawa M, Juhani Airaksinen KE, Assmann G, Becker CR, Chesebro JH, Farb A, Galis ZS, Jackson C, Jang IK, Koenig W, Lodder RA, March K, Demirovic J, Navab M, Priori SG, Rekhter MD, Bahr R, Grundy SM, Mehran R, Colombo A, Boerwinkle E, Ballantyne C, Insull W Jr, Schwartz RS, Vogel R, Serruys PW, Hansson GK, Faxon DP, Kaul S, Drexler H, Greenland P, Muller JE, Virmani R, Ridker PM, Zipes DP, Shah PK, Willerson JT. From vulnerable plaque to vulnerable patient: a call for new definitions and risk assessment strategies: part I. *Circulation*. 2003;108:1664–1672. doi: 10.1161/01.CIR.0000087480.94275.97.
- Libby P. Inflammation in atherosclerosis. *Nature*. 2002;420:868–874. doi: 10.1038/nature01323.
- Silvestre-Roig C, de Winther MP, Weber C, Daemen MJ, Lutgens E, Soehnlein O. Atherosclerotic plaque destabilization: mechanisms, models, and therapeutic strategies. *Circ Res*. 2014;114:214–226. doi: 10.1161/CIRCRESAHA.114.302355.
- Rudd JH, Warburton EA, Fryer TD, Jones HA, Clark JC, Antoun N, Johnström P, Davenport AP, Kirkpatrick PJ, Arch BN, Pickard JD, Weissberg PL. Imaging atherosclerotic plaque inflammation with [18F]-fluorodeoxyglucose positron emission tomography. *Circulation*. 2002;105:2708–2711.
- Tawakol A, Migrino RQ, Bashian GG, Bedri S, Vermylen D, Cury RC, Yates D, LaMuraglia GM, Furie K, Houser S, Gewirtz H, Muller JE, Brady TJ, Fischman AJ. *In vivo* 18F-fluorodeoxyglucose positron emission tomography imaging provides a noninvasive measure of carotid plaque inflammation in patients. *J Am Coll Cardiol*. 2006;48:1818–1824. doi: 10.1016/j.jacc.2006.05.076.
- Figuerola AL, Subramanian SS, Cury RC, Truong QA, Gardecki JA, Tearney GJ, Hoffmann U, Brady TJ, Tawakol A. Distribution of inflammation within carotid atherosclerotic plaques with high-risk morphological features: a comparison between positron emission tomography activity, plaque morphology, and histopathology. *Circ Cardiovasc Imaging*. 2012;5:69–77. doi: 10.1161/CIRCIMAGING.110.959478.
- Tahara N, Kai H, Yamagishi S, Mizoguchi M, Nakaura H, Ishibashi M, Kaida H, Baba K, Hayabuchi N, Imaizumi T. Vascular inflammation evaluated by [18F]-fluorodeoxyglucose positron emission tomography is associated with the metabolic syndrome. *J Am Coll Cardiol*. 2007;49:1533–1539. doi: 10.1016/j.jacc.2006.11.046.
- Kim TN, Kim S, Yang SJ, Yoo HJ, Seo JA, Kim SG, Kim NH, Baik SH, Choi DS, Choi KM. Vascular inflammation in patients with impaired glucose tolerance and type 2 diabetes: analysis with 18F-fluorodeoxyglucose positron emission tomography. *Circ Cardiovasc Imaging*. 2010;3:142–148. doi: 10.1161/CIRCIMAGING.109.888909.
- Kwee RM, Truijman MT, Mess WH, Teule GJ, ter Berg JW, Franke CL, Korten AG, Meems BJ, Prins MH, van Engelshoven JM, Wildberger JE, van Oostenbrugge RJ, Kooi ME. Potential of integrated [18F] fluorodeoxyglucose positron-emission tomography/CT in identifying vulnerable carotid plaques. *AJNR Am J Neuroradiol*. 2011;32:950–954. doi: 10.3174/ajnr.A2381.
- Müller HF, Viacoz A, Fisch L, Bonvin C, Lovblad KO, Ratib O, Lalive P, Pagano S, Vuilleumier N, Willi JP, Sztajzel R. 18FDG-PET-CT: an imaging biomarker of high-risk carotid plaques. Correlation to symptoms and microembolic signals. *Stroke*. 2014;45:3561–3566. doi: 10.1161/STROKEAHA.114.006488.
- Izquierdo-Garcia D, Davies JR, Graves MJ, Rudd JH, Gillard JH, Weissberg PL, Fryer TD, Warburton EA. Comparison of methods for magnetic resonance-guided [18-F]fluorodeoxyglucose positron emission tomography in human carotid arteries: reproducibility, partial volume correction, and correlation between methods. *Stroke*. 2009;40:86–93. doi: 10.1161/STROKEAHA.108.521393.
- Buettner C, Rudd JH, Fayad ZA. Determinants of FDG uptake in atherosclerosis. *JACC Cardiovasc Imaging*. 2011;4:1302–1304. doi: 10.1016/j.jcmg.2011.09.011.
- Bucerius J, Mani V, Moncrieff C, Machac J, Fuster V, Farkouh ME, Tawakol A, Rudd JH, Fayad ZA. Optimizing 18F-FDG PET/CT imaging of vessel wall inflammation: the impact of 18F-FDG circulation time, injected dose, uptake parameters, and fasting blood glucose levels. *Eur J Nucl Med Mol Imaging*. 2014;41:369–383. doi: 10.1007/s00259-013-2569-6.
- Boggs KP, Rock CO, Jackowski S. Lysophosphatidylcholine and 1-O-octadecyl-2-O-methyl-rac-glycero-3-phosphocholine inhibit the CDP-choline pathway of phosphatidylcholine synthesis at the CTP:phosphocholine cytidyltransferase step. *J Biol Chem*. 1995;270:7757–7764.
- Mertens K, Slaets D, Lambert B, Acou M, De Vos F, Goethals I. PET with (18F)-labelled choline-based tracers for tumour imaging: a review of the literature. *Eur J Nucl Med Mol Imaging*. 2010;37:2188–2193. doi: 10.1007/s00259-010-1496-z.
- Roivainen A, Parkkola R, Yli-Kerttula T, Lehtikainen P, Viljanen T, Mötönen T, Nuutila P, Minn H. Use of positron emission tomography with methyl-11C-choline and 2-18F-fluoro-2-deoxy-D-glucose in comparison with magnetic resonance imaging for the assessment of inflammatory proliferation of synovium. *Arthritis Rheum*. 2003;48:3077–3084. doi: 10.1002/art.11282.
- Wyss MT, Weber B, Honer M, Späth N, Ametamey SM, Westera G, Bode B, Kaim AH, Buck A. 18F-choline in experimental soft tissue infection assessed with autoradiography and high-resolution PET. *Eur J Nucl Med Mol Imaging*. 2004;31:312–316. doi: 10.1007/s00259-003-1337-4.



20. Matter CM, Wyss MT, Meier P, Späth N, von Lukowicz T, Lohmann C, Weber B, Ramirez de Molina A, Laca JC, Ametamey SM, von Schulthess GK, Lüscher TF, Kaufmann PA, Buck A. 18F-choline images murine atherosclerotic plaques ex vivo. *Arterioscler Thromb Vasc Biol.* 2006;26:584–589. doi: 10.1161/01.ATV.0000200106.34016.18.
21. Laitinen IE, Luoto P, Någren K, Marjamäki PM, Silvola JM, Hellberg S, Laine VJ, Ylä-Herttua S, Knuuti J, Roivainen A. Uptake of 11C-choline in mouse atherosclerotic plaques. *J Nucl Med.* 2010;51:798–802. doi: 10.2967/jnumed.109.071704.
22. Kato K, Schober O, Ikeda M, Schäfers M, Ishigaki T, Kies P, Naganawa S, Stegger L. Evaluation and comparison of 11C-choline uptake and calcification in aortic and common carotid arterial walls with combined PET/CT. *Eur J Nucl Med Mol Imaging.* 2009;36:1622–1628. doi: 10.1007/s00259-009-1152-7.
23. Grant EG, Benson CB, Moneta GL, Alexandrov AV, Baker JD, Bluth EI, Carroll BA, Eliasziw M, Gocke J, Hertzberg BS, Katanick S, Needleman L, Pellerito J, Polak JF, Rholl KS, Wooster DL, Zierler RE. Carotid artery stenosis: gray-scale and Doppler US diagnosis—Society of Radiologists in Ultrasound Consensus Conference. *Radiology.* 2003;229:340–346. doi: 10.1148/radiol.2292030516.
24. DeGrado TR, Reiman RE, Price DT, Wang S, Coleman RE. Pharmacokinetics and radiation dosimetry of 18F-fluorocholine. *J Nucl Med.* 2002;43:92–96.
25. Taqueti VR, Di Carli MF, Jerosch-Herold M, Sukhova GK, Murthy VL, Folco EJ, Kwong RY, Ozaki CK, Belkin M, Nahrendorf M, Weissleder R, Libby P. Increased microvascularization and vessel permeability associate with active inflammation in human atheromata. *Circ Cardiovasc Imaging.* 2014;7:920–929. doi: 10.1161/CIRCIMAGING.114.002113.
26. Sluimer JC, Kolodgie FD, Bijnens AP, Maxfield K, Pacheco E, Kutys B, Duimel H, Frederik PM, van Hinsbergh VW, Virmani R, Daemen MJ. Thin-walled microvessels in human coronary atherosclerotic plaques show incomplete endothelial junctions relevance of compromised structural integrity for intraplaque microvascular leakage. *J Am Coll Cardiol.* 2009;53:1517–1527. doi: 10.1016/j.jacc.2008.12.056.
27. Folco EJ, Sheikine Y, Rocha VZ, Christen T, Shvartz E, Sukhova GK, Di Carli MF, Libby P. Hypoxia but not inflammation augments glucose uptake in human macrophages: implications for imaging atherosclerosis with 18fluorine-labeled 2-deoxy-D-glucose positron emission tomography. *J Am Coll Cardiol.* 2011;58:603–614. doi: 10.1016/j.jacc.2011.03.044.
28. Bucnerius J, Schmaljohann J, Böhm I, Palmedo H, Gohlke S, Tiemann K, Schild HH, Biersack HJ, Manka C. Feasibility of 18F-fluoromethylcholine PET/CT for imaging of vessel wall alterations in humans—first results. *Eur J Nucl Med Mol Imaging.* 2008;35:815–820. doi: 10.1007/s00259-007-0685-x.
29. Förster S, Rominger A, Saam T, Wolpers S, Nikolaou K, Cumming P, Reiser MF, Bartenstein P, Hacker M. 18F-fluoroethylcholine uptake in arterial vessel walls and cardiovascular risk factors: correlation in a PET-CT study. *Nuklearmedizin.* 2010;49:148–153. doi: 10.3413/nukmed-0299.
30. Brandl R, Richter T, Haug K, Wilhelm MG, Maurer PC, Nathrath W. Topographic analysis of proliferative activity in carotid endarterectomy specimens by immunocytochemical detection of the cell cycle-related antigen Ki-67. *Circulation.* 1997;96:3360–3368.
31. Beckmann J, Schubert J, Morhenn HG, Grau V, Schnettler R, Lips KS. Expression of choline and acetylcholine transporters in synovial tissue and cartilage of patients with rheumatoid arthritis and osteoarthritis. *Cell Tissue Res.* 2015;359:465–477. doi: 10.1007/s00441-014-2036-0.
32. Davies JR, Izquierdo-Garcia D, Rudd JH, Figg N, Richards HK, Bird JL, Aigbirhio FI, Davenport AP, Weissberg PL, Fryer TD, Warburton EA. FDG-PET can distinguish inflamed from non-inflamed plaque in an animal model of atherosclerosis. *Int J Cardiovasc Imaging.* 2010;26:41–48. doi: 10.1007/s10554-009-9506-6.
33. Menezes LJ, Kotze CW, Agu O, Richards T, Brookes J, Goh VJ, Rodriguez-Justo M, Endozo R, Harvey R, Yusuf SW, Ell PJ, Groves AM. Investigating vulnerable atheroma using combined (18F-FDG PET/CT angiography of carotid plaque with immunohistochemical validation. *J Nucl Med.* 2011;52:1698–1703. doi: 10.2967/jnumed.111.093724.
34. Shaikh S, Welch A, Ramalingam SL, Murray A, Wilson HM, McKiddie F, Brittenden J. Comparison of fluorodeoxyglucose uptake in symptomatic carotid artery and stable femoral artery plaques. *Br J Surg.* 2014;101:363–370. doi: 10.1002/bjs.9403.
35. Dweck MR, Chow MW, Joshi NV, Williams MC, Jones C, Fletcher AM, Richardson H, White A, McKillip G, van Beek EJ, Boon NA, Rudd JH, Newby DE. Coronary arterial 18F-sodium fluoride uptake: a novel marker of plaque biology. *J Am Coll Cardiol.* 2012;59:1539–1548. doi: 10.1016/j.jacc.2011.12.037.
36. Joshi NV, Vesey AT, Williams MC, Shah AS, Calvert PA, Craighead FH, Yeoh SE, Wallace W, Salter D, Fletcher AM, van Beek EJ, Flapan AD, Uren NG, Behan MW, Cruden NL, Mills NL, Fox KA, Rudd JH, Dweck MR, Newby DE. 18F-fluoride positron emission tomography for identification of ruptured and high-risk coronary atherosclerotic plaques: a prospective clinical trial. *Lancet.* 2014;383:705–713. doi: 10.1016/S0140-6736(13)61754-7.
37. Beer AJ, Pelisek J, Heider P, Saraste A, Reeps C, Metz S, Seidl S, Kessler H, Wester HJ, Eckstein HH, Schwaiger M. PET/CT imaging of integrin  $\alpha v \beta 3$  expression in human carotid atherosclerosis. *JACC Cardiovasc Imaging.* 2014;7:178–187. doi: 10.1016/j.jcmg.2013.12.003.
38. Truijman MT, de Rotte AA, Aaslid R, van Dijk AC, Steinbuch J, Liem MI, Schreuder FH, van der Steen AF, Daemen MJ, van Oostenbrugge RJ, Wildberger JE, Nederkoorn PJ, Hendrikse J, van der Lugt A, Kooi ME, Mess WH. Intraplaque hemorrhage, fibrous cap status, and microembolic signals in symptomatic patients with mild to moderate carotid artery stenosis: the Plaque at RISK study. *Stroke.* 2014;45:3423–3426. doi: 10.1161/STROKEAHA.114.006800.

### CLINICAL PERSPECTIVE

Given limitations of conventional  $^{18}\text{F}$ -fluoro-2-deoxy-D-glucose positron emission tomography-computed tomography ( $^{18}\text{F}$ -FDG PET-CT) imaging, the main inflammation-sensitive molecular imaging agent used for clinical molecular imaging of atherosclerosis, the search for new tracers with improved pharmacokinetics or specificity are important. The present article hypothesizes that  $^{18}\text{F}$ -fluorocholine ( $^{18}\text{F}$ -FCH) PET imaging is a valuable imaging tool for the identification of intraplaque inflammation and identification of vulnerable plaques. As proof-of-principle, the article describes the use of  $^{18}\text{F}$ -FCH PET-CT for diagnosing carotid vulnerable plaques in patients with symptomatic carotid stenosis. The present data provide evidence that  $^{18}\text{F}$ -FCH is highly taken up in symptomatic plaques, while it shows no or significantly less uptake in asymptomatic ones. Importantly,  $^{18}\text{F}$ -FCH uptake significantly correlates with the intraplaque macrophage content. This is a novel aspect proving that  $^{18}\text{F}$ -FCH PET-CT imaging can be used to detect vulnerable, inflamed atherosclerotic plaques in symptomatic patients. A major advantage of this modality over that of conventional  $^{18}\text{F}$ -FDG PET imaging is that  $^{18}\text{F}$ -FCH quickly clears from blood without any necessary glucose modulation and it accumulates in inflamed atherosclerotic plaques to achieve a reasonable target to background ratio in a short time. This demonstration makes  $^{18}\text{F}$ -FCH an attractive imaging tracer compared with  $^{18}\text{F}$ -FDG that could allow for high throughput diagnostic imaging in clinics. The present study highlights the important potential clinical utility of the tracer studied.